Kazanna C. Hames,[1] Adrian Vella,[1] Bradley J. Kemp,[2] and Michael D. Jensen[1]

Free Fatty Acid Uptake in Humans With CD36 Deficiency

Diabetes 2014;63:3606–3614 | DOI: 10.2337/db14-0369

Animal models have demonstrated that CD36 facilitates cell membrane free fatty acid (FFA) transport, but its role in human metabolism is not well understood. We measured heart, liver, adipose (three depots), and muscle (truncal postural and thigh locomotive) FFA uptake using [^{11}C]palmitate positron emission tomography (PET) scans in a family of five carrying the Pro90Ser CD36 mutation (2 homozygotes had no CD36) and matched control volunteers. PET scans were done under conditions of suppressed and slightly increased palmitate concentrations. During suppressed palmitate conditions, muscle and adipose palmitate uptake were markedly reduced in homozygotes but not heterozygotes for the Pro90Ser CD36 mutation, whereas when palmitate concentration was slightly increased, uptake in muscle and adipose did not differ between control subjects and homozygous family members. Hepatic FFA uptake was similar in all participants regardless of palmitate concentrations, whereas myocardial FFA uptake was diminished in the Pro90Ser homozygotes during both suppressed and increased palmitate conditions. We conclude that CD36 *1*) facilitates FFA transport into muscle and adipose tissue in humans when extracellular concentrations are reduced but not when they are modestly elevated, *2*) is not rate limiting for hepatic FFA uptake, and *3*) is needed for normal cardiac FFA uptake over a range of FFA concentrations from low to slightly elevated.

Free fatty acids (FFAs), the products of adipose tissue lipolysis, are critical molecules for many tissues as a source of fuel, membrane synthesis, and signaling molecules. The mechanism(s) by which circulating FFA enter cells for further metabolism is not completely understood. CD36, the human analog of fatty acid transporter, is a glycoprotein that is present in the plasma membrane of many cell types (1). It functions as a scavenger receptor for various ligands (2) and facilitates the inward transport of fatty acids (3,4). The role of CD36 in long-chain FFA metabolism (binding/transport) was suggested 20 years ago (5) and further clarified using whole animal and tissue experiments from *CD36* knockout mice (3,6–8). Results from ex vivo experiments suggest that CD36 is more important for cellular FFA uptake when the FFA-to-albumin ratio is low (e.g., low unbound FFA concentrations) (3). Whether CD36 also supports inward fatty acid transport when FFA concentrations are increased in vivo is not clear, and its role in human physiology is also not well documented. Therapeutic strategies aimed at inhibiting CD36-mediated fatty acid transport are being developed (9), making it important to understand the tissues and circumstances where such interventions might be effective.

The majority of research examining the role of CD36 in humans has been conducted in Asian populations who have a higher prevalence of a gene variant that, in homozygotes, results in expression of a nonfunctioning variant of CD36 (10–12). Associations between CD36 deficiency and insulin resistance (13), dyslipidemia (14), and cardiovascular health (15) have been published. We are aware of three reports of reduced or absent myocardial fatty acid uptake in patients with documented (16,17) or presumed (18) *CD36* gene mutations. Little else is known about the possible role of CD36 in extracardiac tissue FFA uptake in humans.

Serendipitously, a volunteer for one of our FFA metabolism studies had undetectable adipose tissue CD36 content. This study participant was of Asian descent and agreed to undergo testing for *CD36* mutations; testing showed that he was homozygous for the C478T substitution in *CD36* resulting in a Pro90Ser substitution. All four of the participant's immediate, adult

[1]Endocrine Research Unit, Mayo Clinic, Rochester, MN
[2]Department of Nuclear Medicine, Mayo Clinic, Rochester, MN
Corresponding author: Michael D. Jensen, jensen@mayo.edu.
Received 3 March 2014 and accepted 5 June 2014.

family members agreed to be tested for the Pro90Ser CD36 mutation. and all five family members agreed to undergo the [^{11}C]palmitate, positron emission tomography (PET)/computed tomography (CT) studies outlined below to measure FFA uptake in multiple tissues in vivo. Our objectives were to define the role of CD36 in tissue FFA uptake as a function of plasma FFA concentrations in humans.

RESEARCH DESIGN AND METHODS

The protocol was approved by the Institutional Review Board and conducted at the Center for Translational Science Activities' Clinical Research Unit (CRU) and the Nuclear Medicine Department at Mayo Clinic, Rochester, MN. Written informed consent was obtained from all volunteers.

Participants

Five family members (mother, father, and three children) donated blood for DNA analysis of the gene alteration resulting in the Pro90Ser mutation of CD36. Both parents and one daughter were heterozygous, whereas the other daughter and son were homozygous. To optimize the planned comparisons of tissue FFA uptake, we recruited volunteers matched to each family member by sex, age (± 2 years), BMI (±1.0 kg/m^2), and body fat (±3%). We recruited a Caucasian control population because of their very low prevalence of *CD36* gene mutations (0.22%) (10).

Study Protocol

Prior to the PET/CT studies, body composition was measured using DEXA (GE Lunar; General Electric, Madison, WI). We also performed biopsies of subcutaneous adipose tissue from the abdomen and thigh (19) to measure fat cell size, CD36 protein content, and the activities of some enzymes involved in fatty acid storage: Acyl-CoA synthetase (ACS) and diacylglycerol acetyltransferase (DGAT).

Each participant completed two [^{11}C]palmitate PET studies to measure tissue FFA uptake. The studies were designed to create FFA concentrations below and above those typically observed in overnight postabsorptive adults. The studies were scheduled at least 1 week apart, and the order of the studies was assigned by random chance. Participants were asked to maintain their usual eating and physical activity habits between visits and not to participate in vigorous physical activity for the 3 days prior to these visits. For suppression of FFA concentrations, the participants were instructed to consume breakfast before reporting for the study. In addition, prior to the PET/CT scan they consumed a 75-g glucose beverage and received a continuous intravenous infusion of 20% dextrose at a rate of 5 mg · kg fat-free mass^{-1} · min^{-1} throughout the study. To create increased blood FFA concentrations, we instructed participants to abstain from consuming anything other than water for at least 18 h prior to admission to the visit. For both studies, an intravenous catheter was placed in an antecubital vein for administration of infusates and a retrograde catheter was inserted in a hand vein of the opposite arm to collect arterialized venous blood using a "hot box" technique. Blood samples were collected to measure plasma FFA, glucose, and insulin prior to consumption of glucose and/or the start of any infusions.

A CT scan of the trunk was completed, followed immediately by a 20-min, dynamic [1-^{11}C]palmitate PET scan to measure palmitate uptake in truncal tissues and organs. All studies were conducted using a Discovery RX PET/CT system (GE Healthcare, Waukesha, WI) operating in two-dimensional mode. The PET system used the following sequence after a bolus injection of the [1-^{11}C]palmitate (~1,110 MBq, 20–30 mCi) to measure the spatial and temporal distribution of the tracer: 20 frames at 3 s, 12 frames at 10 s, 4 frames at 20 s, and 4 frames at 300 s. Blood samples (3–10 mL) were collected at 6, 10, 14, 18, 20, and 22 min to correct the time activity curve (TAC) for $^{11}CO_2$ (see procedure below) and to measure plasma palmitate concentrations. After completion of the dynamic scan, a CT scan and static PET scan of the upper thigh were performed to determine tissue palmitate uptake of that region.

Materials

[U-^{13}C]palmitate was purchased from Cambridge Isotope Laboratories, Andover, MA. [1-^{11}C]palmitate was synthesized by the Nuclear Medicine PET Radiochemistry Laboratory of the Mayo Clinic using previously described techniques (20,21).

Analyses

DNA Analysis

Genomic DNA was extracted from whole EDTA blood of each family member using a Qiagen Gentra Puregene blood kit. PCR DNA sequencing was used to detect the C478T substitution in *CD36*.

Sample Analyses

Adipose tissue samples were thoroughly rinsed of blood with saline. A portion of the sample was placed in HEPES buffer and used to measure cell size after collagenase digestion as previously described (22). An aliquot of the biopsy sample was flash frozen and stored at −80°C until assayed for CD36 content (23), as well as ACS and DGAT enzyme activities (24).

Plasma palmitate concentrations were measured by ultra-performance liquid chromatography using a modification of our high-performance liquid chromatography procedure (25). Plasma concentrations were converted to whole blood concentration using each individual's hematocrit. Plasma palmitate enrichments were measured by liquid chromatography/mass spectrometry (26) to calculate palmitate clearance as previously described (27).

The following procedure was adapted from the methods of Fox et al. (28) and Bergmann et al. (29) to correct for the contribution of metabolized tracer (in the form of $^{11}CO_2$) to the total radioactivity measured in left ventricle

(LV) cavity blood to create the input function. From the blood samples collected during the dynamic PET scan, pairs of 1-mL aliquots of blood from each time point were placed into scintillation tubes containing 3 mL isopropyl alcohol. One milliliter of 6 N HCl was added to one aliquot and bubbled for 10 min with air to release CO_2, and 1 mL 0.1 NaOH was added to the other aliquot. Radioactivity in the samples was measured with a γ-well counter. Total ^{11}C radioactivity (kilobecquerels per milliliter) was measured in the alkalinized aliquot, and non$^{11}CO_2$ radioactivity (i.e., palmitate) was measured in the acidified aliquot. The ratio of the non$^{11}CO_2$ radioactivity to the alkalinized aliquot from each pair was corrected for isotopic decay.

PET/CT Image Analysis

All PET images were reconstructed with an iterative ordered subset expectation maximization reconstruction algorithm and a Gaussian postfilter of 7 mm. Corrections for attenuation, scatter, dead time, and randoms were applied; all frames were decay corrected to the start of the acquisition. The PET/CT images were transferred to PMOD (version 2.8; PMOD Technologies, Zurich, Switzerland). The CT provided borders to tissue, organs, and bone structures to define regions of interest (ROI) in the LV cavity and LV myocardium, liver, trunk postural muscles (i.e., erector spinae, abdominal oblique muscles, transversus abdominis, and rectus abdominis), and abdominal subcutaneous and visceral adipose tissue, as well as thigh adipose tissue and muscles of locomotion (i.e., quadriceps and hamstrings). The influx constant (K_i) was determined using the Patlak analysis of the TACs generated for each ROI in the trunk (30). The blood input function was derived from a TAC using the ROI in the LV cavity combined with results from the blood samples corrected for the $^{11}CO_2$ content. K_i (milliliters per gram tissue per minute) was then multiplied by the palmitate concentration in blood (micromoles per milliliter) to give the FFA uptake rate of each tissue (micromoles per gram tissue per minute). The FFA uptake rates in thigh adipose tissue and muscle from the static PET images were measured as follows: standardized uptake values (SUVs), which represent the uptake in an ROI normalized by the amount of radioactivity administered per body weight, were calculated for thigh muscle and adipose tissue regions of the static image of the thigh. The FFA uptake rate in thigh muscle was calculated by scaling the FFA uptake in truncal postural muscle by the ratio of the SUV in thigh muscle to the SUV in each individual's truncal postural muscle, where the SUV in trunk postural muscle was calculated from the final frame of the dynamic scan. Similarly, the FFA uptake rate in thigh adipose tissue was calculated by scaling the FFA uptake in each individual's abdominal adipose tissue by the ratio of SUV in thigh adipose tissue to the SUV in abdominal adipose tissue. This approach assumes that the relative FFA uptake rates for thigh and truncal muscles are equal to the relative SUVs for the thigh and truncal skeletal muscle. A similar assumption is made for thigh and truncal adipose tissue.

Statistical Analyses

Normally distributed data are expressed as means ± SD, and nonnormally distributed data are expressed as medians with interquartile intervals (25th, 75th). Two-sample *t* tests were used to compare differences in normally distributed, random variables between groups. We tested whether K_i could be used as a stand-alone, independent variable to compare between groups but found that K_i values were positively correlated with blood palmitate concentrations. Because of the strong, positive correlation between plasma FFA concentrations and adipose FFA storage (31,32), we examined the relationships between blood palmitate concentrations and tissue FFA uptake rates measured by PET. For each tissue, we examined whether there was a linear relationship between blood palmitate concentrations and FFA uptake rates for low and high FFA conditions separately. Multiple linear regression analyses were used to relate palmitate uptake in each ROI during both study days to plasma palmitate concentration. The Cook D value, as well as visual inspection of the regression and leverage plots, showed that the Pro90Ser homozygous participants were consistent outliers during low plasma FFA conditions for palmitate uptake rates in all ROIs except liver. With the additional knowledge that these participants were Pro90Ser homozygous for the *CD36* gene and had no measurable CD36 in adipose tissue, the homozygous subjects' data were therefore excluded from the regression model predicting palmitate uptake in myocardium, abdominal and femoral subcutaneous adipose tissue, visceral adipose tissue, and postural and locomotive skeletal muscle in relation to plasma palmitate concentrations during the low-FFA condition. Thus, for the low-FFA condition, we used data from the control participants (n = 5) and the Pro90Ser heterozygous family members (n = 3) with readily detectable adipose CD36 protein content to determine the linear fit. The data from the two Pro90Ser homozygous family members with undetectable adipose CD36 were assessed relative to the results from the CD36-sufficient group (see RESULTS). $P < 0.05$ was considered statistically significant. JMP 9.0.1 (SAS Institute, Cary, NC) was used to run the analyses.

RESULTS

Subject characteristics are provided in Table 1. CD36 protein was undetectable in abdominal and femoral subcutaneous adipose tissue of the Pro90Ser homozygotes. CD36 was measurable in adipose tissue from the Pro90Ser heterozygous family members and was ~40–60% less than that found in control subjects (Table 1). ACS and DGAT activities in abdominal and femoral adipose tissue were not different between family members and control subjects. The median plasma leptin concentrations for family members (n = 5) was 4.3 ng/mL (interquartile intervals 2.1, 4.9) and for the control subjects (n = 5) was 4.8 ng/mL (2.4, 9.1). There was a strong, positive relationship between plasma leptin concentrations and percent body

Table 1—Subject characteristics

	CD36-deficient: homozygous family members	CD36-sufficient		
		Heterozygous family members	Control subjects	*P*
n	2	3	5	
Sex (male/female)	1/1	1/2	2/3	
Age (years)	25/22	41 ± 20	34 ± 16	
BMI (kg/m^2)	22.6/21.4	21.8 ± 1.2	22.3 ± 1.8	
Body fat (%)	19/24	28 ± 6	24 ± 6	
Abdominal subcutaneous adipose tissue				
Adipocyte size (μg/cell)	0.59/0.92	0.79 ± 0.21	0.29 ± 0.09	0.003
CD36 (arbitrary units/mg tissue)		6.3 ± 4.5	10.6 ± 2.9	0.23
ACS (pmol/min/mg tissue)	64/57	61 ± 22	71 ± 20	0.40
DGAT (pmol/min/mg tissue)	5.8/10.9	8.6 ± 2.8	7.3 ± 1.5 (*n* = 4)	0.41
Thigh subcutaneous adipose tissue				
Adipocyte size (μg lipid/cell)	0.36/0.78	0.73 ± 0.32	0.72 ± 0.33	0.80
CD36 (arbitrary units/mg tissue)		4.9 ± 2.2	11.5 ± 4.7	0.04
ACS (pmol/min/mg tissue)	61/56	56 ± 20	87 ± 24	0.05
DGAT (pmol/min/mg tissue)	4.5/10.9	9.8 ± 4.3	8.7 ± 2.4	0.92

The normally distributed data, presented as means ± SD, are from family members (n = 5) and control subjects (n = 5) unless otherwise noted. The individual data for the two homozygous Pro90Ser family members are provided. Age, BMI, and body fat were intentionally matched and thus not subject to statistical testing.

fat (P = 0.007) as expected (33); the relationship was not different between family members and control subjects.

Eighteen hours of fasting on the high-FFA study day resulted in plasma glucose and insulin concentrations of 4.3 ± 0.4 mmol/L and 2.7 ± 1.9 μU/mL, respectively, and plasma and whole blood palmitate concentrations of 145 ± 34 and 84 ± 20 μmol/L, respectively. The glucose drink and intravenous glucose given to achieve the low-FFA condition resulted in plasma glucose and insulin concentrations of 8.8 ± 2.0 mmol/L and 41.7 ± 16.6 μU/mL, respectively, and plasma and whole blood palmitate concentrations of 19 ± 14 and 11 ± 8 μmol/L, respectively.

Because the three Pro90Ser heterozygous family members and control subjects had detectable CD36 protein and because the relationships between blood palmitate concentrations and tissue palmitate uptake rates were indistinguishable between heterozygous family members and control subjects, the data from these eight participants were used to represent the CD36-sufficient group. The two Pro90Ser homozygous family members are referred to as CD36-deficient participants.

For the CD36-sufficient participants, muscle and adipose palmitate uptake rates as a function of blood palmitate concentrations under high-FFA conditions are shown in Fig. 1. The positive relationships between blood palmitate concentrations and rates of palmitate uptake in trunk and thigh muscles, as well as for abdominal subcutaneous adipose tissue, were highly significant, whereas these relationships were of borderline significance for femoral and visceral adipose tissue (Fig. 1). There were also strong, positive relationships between blood palmitate concentrations and palmitate uptake in liver (Fig. 2*A*) and myocardium (Fig. 3*A*). Our hypothesis that CD36 deficiency would reduce myocardial palmitate uptake was consistent with the data from the high-FFA study day: myocardial palmitate uptake rates were >2 SD below predicted for blood palmitate concentrations. In contrast, for all noncardiac tissues (Figs. 1 and 2*A*) the CD36-deficient participants were indistinguishable from the CD36-sufficient participants. The palmitate uptake rates in CD36-deficient participants were as likely to be greater as they were to be less than those seen in the CD36-sufficient group. These results suggest that CD36 is important for normal myocardial FFA uptake but does not limit liver, muscle, and adipose FFA uptake when FFA concentrations are modestly greater than those typically seen in overnight postabsorptive adults.

Figures 2*B*, 3*B*, and 4 depict the relationships between blood palmitate concentrations and PET-measured tissue palmitate uptake rates for the CD36-sufficient and -deficient participants under low-FFA conditions. All associations between blood palmitate concentrations and tissue palmitate uptake rates for CD36-sufficient participants were highly statistically significant. Hepatic palmitate uptake is clearly identical in CD36-deficient and -sufficient participants (Fig. 2*B*). However, myocardial, adipose tissue, and muscle palmitate uptake rates for CD36-deficient participants were uniformly less than those predicted for the CD36-sufficient participants (Figs. 3*B* and 4). To quantify the differences in tissue palmitate uptake between the CD36-deficient and -sufficient volunteers, we calculated the residual differences (observed–predicted) for each of the CD36-sufficient volunteers and computed the SD of the residual differences. Palmitate uptake rates in CD36-deficient family members were at least >2 SD below that predicted by blood palmitate concentrations of the CD36-sufficient participants for all nonhepatic tissues,

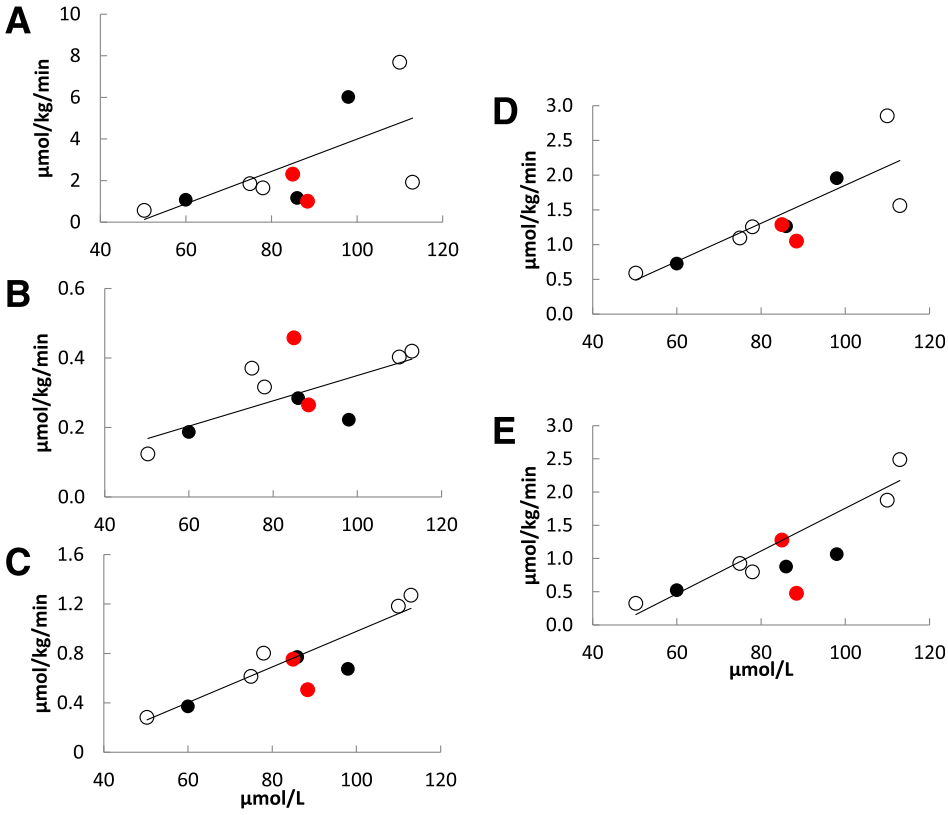

Figure 1—PET-measured palmitate uptake rate as a function of blood palmitate concentration during high-FFA conditions in control subjects (open circles), heterozygous family members (black circles), and homozygous Pro90Ser family members (red circles) for the following regions: visceral adipose (R = 0.67, P = 0.07) (*A*), thigh (R = 0.70, P = 0.06) (*B*), and abdominal subcutaneous adipose (R = 0.94, P = 0.0006) (*C*) tissue, and trunk (R = 0.85, P = 0.007) (*D*) and thigh (*E*) muscle (R = 0.92, P = 0.001).

the single exception being that thigh muscle palmitate uptake was 1 SD below that predicted by palmitate concentration in one CD36-deficient family member; the other CD36-deficient family member had thigh muscle uptake values >2 SD below predicted. These results show that rates of long-chain FFA uptake are significantly reduced in heart and skeletal muscle, as well as in visceral, abdominal subcutaneous, and thigh adipose tissue in CD36-deficient humans when FFA concentrations are low.

We were able to measure palmitate flux and clearance in 8 of the 10 participants using the [U-^{13}C]palmitate infusion approach (26). On the study day with high-FFA concentrations, plasma palmitate clearance of CD36-deficient participants (n = 2; 717 ± 25 mL/min) appeared no different from the CD36-sufficient participants (n = 6; 773 ± 255 mL/min). However, under low-FFA conditions, average palmitate clearance in the CD36-deficient participants was less than half that of the CD36-sufficient participants (972 vs. 1,985 mL/min), consistent with the reduced uptake by myocardium, skeletal muscle, and adipose tissue in those with CD36 deficiency.

DISCUSSION

We used [1-^{11}C]palmitate dynamic and static PET/CT scan techniques to measure liver, adipose, and muscle FFA uptake in two siblings homozygous for the C478T substitution (Pro90Ser) of *CD36*, resulting in an essential knockout of CD36 protein, as well as three heterozygous Pro90Ser family members and five carefully matched control volunteers. Each participant underwent two separate studies, one creating low and one creating modestly increased FFA concentrations. This study design allowed us to determine whether CD36 deficiency reduces heart, skeletal muscle, adipose tissue, and liver FFA uptake under one or both conditions in humans in vivo. Myocardial palmitate uptake in CD36-deficient family members was reduced under both high- and low-FFA conditions. Muscle and adipose tissue FFA uptake were significantly reduced in CD36-deficient family members only under conditions of low plasma FFA. Liver palmitate uptake in CD36-deficient family members was indistinguishable from CD36-sufficient participants under both FFA conditions. These results emphasize the heterogeneity of CD36-dependent inward transport of FFA with respect to tissues and FFA concentrations in humans.

Previous studies of FFA metabolism in humans with *CD36* mutations have focused on heart disease and used FFA tracers that differ structurally from natural FFA (16,17,34,35). Most have reported evidence for reduced myocardial FFA uptake associated with *CD36* mutations,

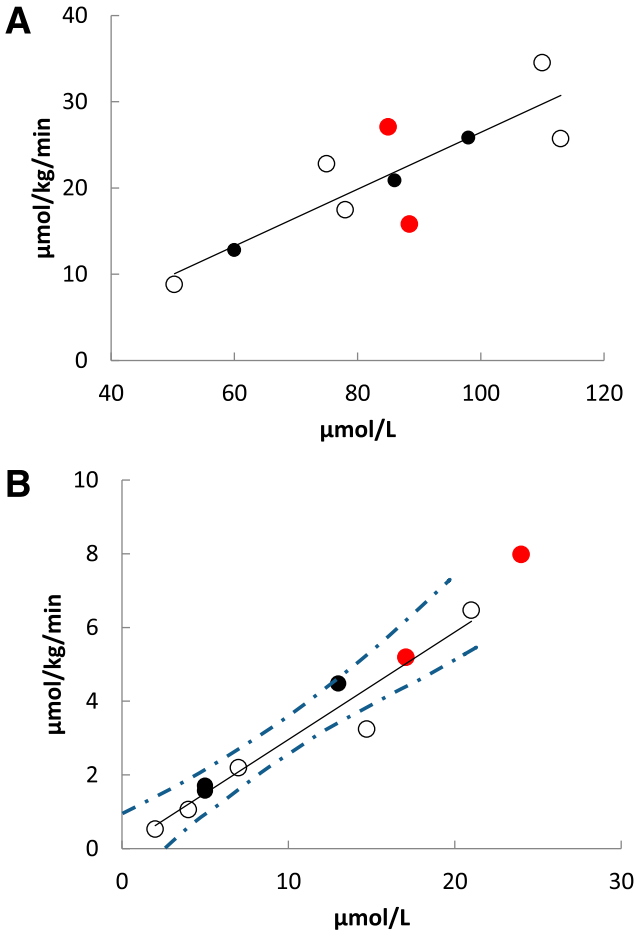

Figure 2—PET-measured rate of palmitate uptake in the liver as a function of blood palmitate concentration at high-FFA (R = 0.92, P = 0.001) (*A*) and low-FFA conditions (R = 0.96, P = 0.0001) (*B*). Control subjects are represented by open circles, heterozygous family members by black circles, and homozygous Pro90Ser family members by red circles. The dashed lines represent the 95% CI around the regression line.

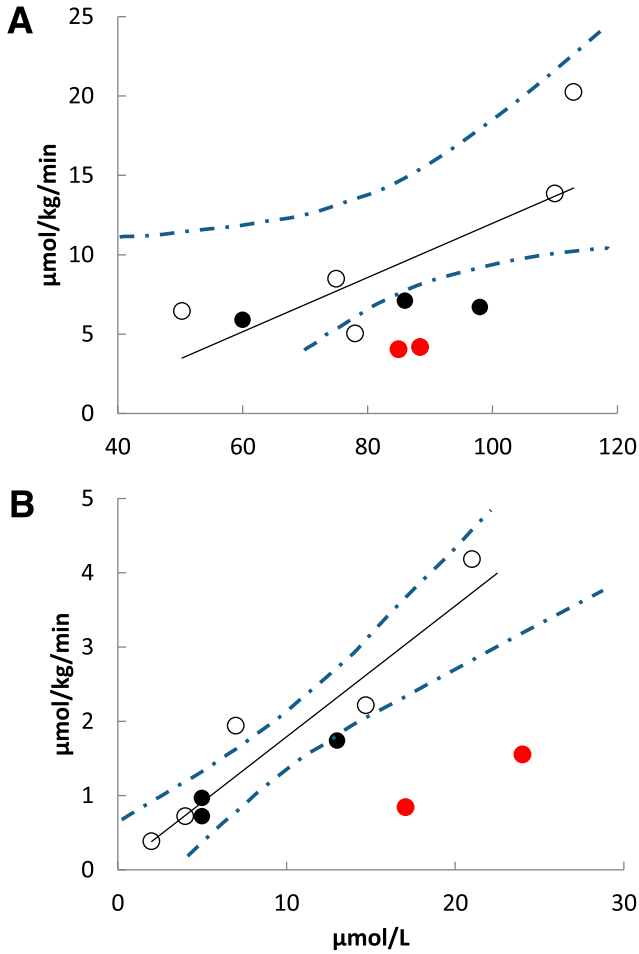

Figure 3—PET-measured myocardial palmitate uptake rate as a function of blood palmitate concentration during high-FFA (*A*) and low-FFA (*B*) conditions in control subjects (open circles), heterozygous family members (black circles), and homozygous Pro90Ser family members (red circles). The concentration/uptake relationships for control subjects plus heterozygous participants were significant for both the high (R = 0.73, P = 0.04) and low (R = 0.94, P = 0.0005) concentrations. The dashed lines represent the 95% CI around the regression line.

but none measured plasma FFA concentrations, which are a major determinant of tissue FFA uptake (32). By using a carbon-labeled palmitate PET tracer and accounting for FFA concentrations, we can confidently conclude that myocardial FFA uptake is dependent to some degree on CD36 under conditions of both high- and low-FFA concentrations. Our results are consistent with the reports of reduced fatty acid uptake in myocardium of humans with *CD36* mutations (16,17,34,35), as well as adipocytes isolated from *CD36* knockout mice under conditions of low, but not high, FFA concentrations (3). However, our results are at odds with a number of experiments using *CD36* knockout mice, including the finding of elevated leptin concentrations (36) and a report of reduced muscle palmitate uptake under normal FFA concentration conditions (37).

In accordance with previous studies (16,17,34,35), we found a 57–73% reduction in myocardial FFA uptake in adults homozygous for the Pro90Ser *CD36* mutation. Given that FFA is an important fuel source for cardiac muscle (38), these combined findings suggest that interventions designed to inhibit CD36 function will reduce myocardial FFA uptake when FFA are high normal or less. Fukuchi et al. (34) observed increased myocardial glucose uptake in concert with reduced FFA uptake in Japanese adults with a *CD36* mutation. Interventions designed to inhibit CD36 function (9) will need to take this into consideration.

We postulate that FFA uptake in adipose and muscle in humans depends to a greater extent upon protein-facilitated inward transport when concentrations of unbound fatty acids are low. Our data strongly suggest that at concentrations equal to or slightly above those seen in the overnight postabsorptive state, fatty acids enter

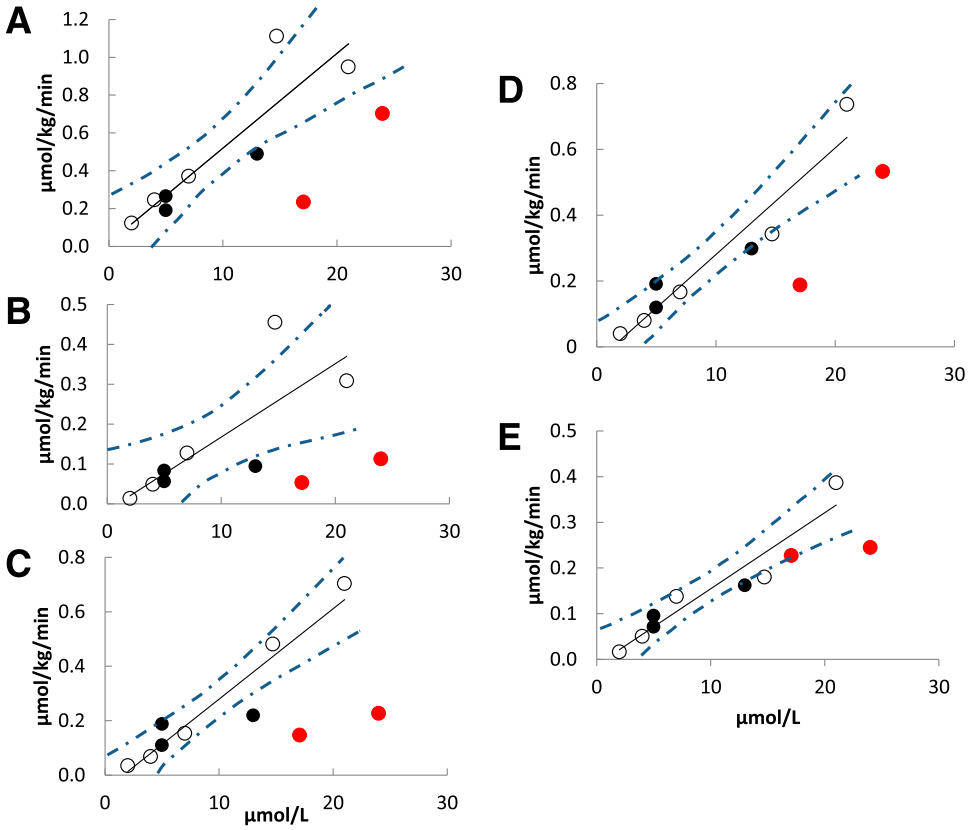

Figure 4—PET-measured palmitate uptake rate as a function of blood palmitate concentration during low-FFA conditions in control subjects (open circles), heterozygous family members (black circles), and homozygous Pro90Ser family members (red circles) for the following regions: visceral adipose (R = 0.91, P = 0.002) (*A*), thigh (R = 0.80, P = 0.02) (*B*), and abdominal subcutaneous adipose (R = 0.95, P = 0.0003) (*C*) tissue, and trunk (R = 0.95, P = 0.0003) (*D*) and thigh (*E*) (R = 0.94, P = 0.0004) muscle. The dashed lines represent the 95% CI around the regression line.

muscle and adipose via passive diffusion (aka flip-flop) or use protein transporters other than CD36. This may indicate that the controversy over facilitated transport versus flip-flop (39) is not an either-or process. Instead, in tissue-specific manners, when extracellular concentrations of unbound fatty acids are low, cells with greater amounts of CD36 and/or other fatty acid transport proteins will be better able to take up fatty acids than those with less (Fig. 5). Consistent with this hypothesis, participants with greater thigh adipose CD36 had greater palmitate uptake in thigh fat than volunteers with lower, but still detectable, CD36 on the low-FFA day (n = 8; r = 0.86, P = 0.01). Conversely, at higher FFA concentrations, cellular fatty acid uptake may be more uniform between different cells/tissues even if they differ substantially in CD36 (40) (Fig. 5). To the extent that there may be competition for fatty acid uptake between FFA and VLDL-derived fatty acids from the action of lipoprotein lipase, it is worthwhile noting that VLDL-triglyceride concentrations are unlikely to be altered by short-term (<2 h) elevations of glucose and insulin compared with fasting (41).

We found that hepatic palmitate uptake in CD36-deficient adults was very similar to CD36-sufficient participants under conditions of both high- and low-FFA concentrations, indicating that the liver does not depend upon CD36-facilitated FFA transport. This finding complements the finding of normal liver (and kidney) uptake of a radioactive iodinated fatty acid analog in postprandial *CD36* knockout mice compared with control mice (7). Many humans, especially in Western societies, spend a considerable portion of the day in the postprandial state with reduced FFA concentrations. In humans with absent or lesser amounts of CD36, postprandial conditions would be expected to favor FFA uptake in tissues such as liver that do not require CD36, resulting in a mild but chronic fatty acid overload relative to muscle and adipose tissue. Our findings may explain the observation of Goudriaan et al. (42), who noted hepatic but not muscle insulin resistance in *CD36* knockout mice, as well as the observation that dyslipidemia, more so than insulin resistance, is associated with *CD36* mutations in humans (43).

There are some limitations to this study. Despite screening a large gene database of Rochester, MN, residents, we were unable to identify anymore individuals with important CD36 polymorphisms, limiting our study to the two CD36-deficient participants. We believe that our conclusions are strong, however, because of the consistency of the data for three adipose tissue depots and two muscle depots.

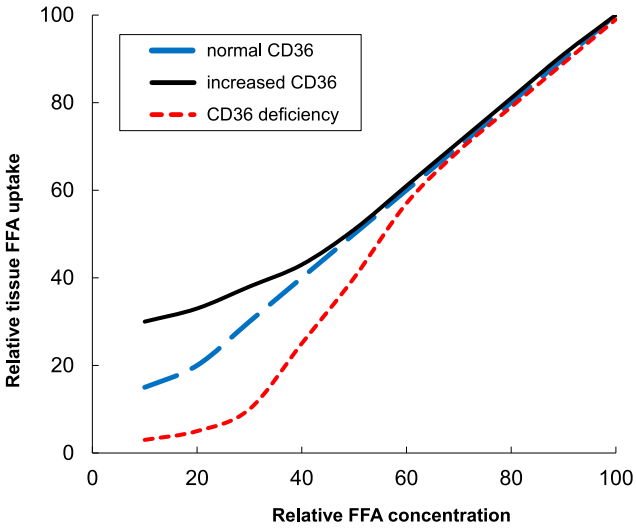

Figure 5—Proposed model for skeletal muscle and adipose tissue FFA uptake in humans. The *x*-axis represents relative FFA concentrations, with 0 being the lowest physiological concentrations that can be achieved and 100 being the highest physiological concentrations that are observed. The *y*-axis represents relative tissue FFA uptake in CD36-dependent tissues, with 0 being the lowest uptake that can be detected and 100 being the highest achievable tissue FFA uptake. In this model, humans with reduced tissue CD36 content will have lesser FFA uptake when FFA concentrations fall below overnight postabsorptive levels, whereas those with increased CD36 content will have greater FFA uptake than predicted based upon plasma FFA concentrations.

Except in liver, palmitate uptake at low concentrations was always below predicted in Pro90Ser homozygotes (usually by >2 SD). The chances that we would observe reduced palmitate uptake of any degree given this number of observations is ~2 in 10,000. Considering the following, we suggest that our evidence is convincing: *1*) the marked degree of the observed defect in comparison with control subjects matched for age, sex, and percent body fat to minimize confounding characteristics; *2*) that our results are biologically plausible; *3*) the very low probability that our findings are by chance; and *4*) that they occur in the context of lesser palmitate clearance during low-FFA concentrations. Our finding that CD36 deficiency results in impaired palmitate uptake in muscle and adipose tissue under conditions of suppressed FFA does not completely address the potential role of other fatty acid transport proteins in humans. However, studies using animal models indicate a minor role for these other FA transporters (e.g., $FABP_{PM}$ and FATP) (37). Likewise, we examined liver, muscle, and adipose palmitate uptake under low and moderately elevated FFA conditions and cannot pinpoint whether there is an exact transition from CD36-facilitated FFA uptake to CD36-independent uptake. Most likely, there is a graduated effect as FFA concentrations decrease. However, performing a large number of PET/CT studies on each volunteer to define their exact response would be problematic owing to the use of ionizing radiation.

In conclusion, we found substantial tissue and FFA concentration-dependent heterogeneity in the requirement for CD36-mediated tissue FFA uptake. CD36 plays an important role in adipose and muscle under conditions of suppressed but not modestly increased FFA concentrations; myocardium appears to use CD36 under both conditions, whereas hepatic FFA uptake is not affected by CD36 deficiency. These findings identify the role of facilitated inward transport for tissue fatty acid metabolism in humans and provide important information when considering CD36 as a therapeutic target (9).

Acknowledgments. The authors are grateful to the participants for playing an integral role in making this research possible. In addition, thanks go out to the Mayo Clinic CRU and Nuclear Medicine staff, and especially Barbara Norby, Carley Vrieze, Christy Allred, Lendia Zhou, Debra Harteneck, and Darlene Lucas, for their technical assistance and help with data collection.

Funding. This work was supported by National Center for Research Resources grant 1-UL1-RR-024150; National Institutes of Health grants DK-45343, DK-40484, and DK-50456; and American Diabetes Association grant 7-12-MN-36.

Duality of Interest. No potential conflicts of interest relevant to this article were reported.

Author Contributions. K.C.H. performed the research, analyzed data, and wrote the manuscript. A.V. designed the research. B.J.K. designed the research and contributed new reagents or analytic tools. M.D.J. designed the research, analyzed data, and wrote the manuscript. M.D.J. is the guarantor of this work and, as such, had full access to all the data in the study and takes responsibility for the integrity of the data and the accuracy of the data analysis.

References

1. Goldberg IJ, Eckel RH, Abumrad NA. Regulation of fatty acid uptake into tissues: lipoprotein lipase- and CD36-mediated pathways. J Lipid Res 2009;50 (Suppl.):S86–S90
2. Hajri T, Abumrad NA. Fatty acid transport across membranes: relevance to nutrition and metabolic pathology. Annu Rev Nutr 2002;22:383–415
3. Febbraio M, Abumrad NA, Hajjar DP, et al. A null mutation in murine CD36 reveals an important role in fatty acid and lipoprotein metabolism. J Biol Chem 1999;274:19055–19062
4. Ibrahimi A, Abumrad NA. Role of CD36 in membrane transport of long-chain fatty acids. Curr Opin Clin Nutr Metab Care 2002;5:139–145
5. Harmon CM, Abumrad NA. Binding of sulfosuccinimidyl fatty acids to adipocyte membrane proteins: isolation and amino-terminal sequence of an 88-kD protein implicated in transport of long-chain fatty acids. J Membr Biol 1993;133: 43–49
6. Bastie CC, Hajri T, Drover VA, Grimaldi PA, Abumrad NA. CD36 in myocytes channels fatty acids to a lipase-accessible triglyceride pool that is related to cell lipid and insulin responsiveness. Diabetes 2004;53:2209–2216
7. Coburn CT, Knapp FF Jr, Febbraio M, Beets AL, Silverstein RL, Abumrad NA. Defective uptake and utilization of long chain fatty acids in muscle and adipose tissues of CD36 knockout mice. J Biol Chem 2000;275:32523–32529
8. Ibrahimi A, Bonen A, Blinn WD, et al. Muscle-specific overexpression of FAT/CD36 enhances fatty acid oxidation by contracting muscle, reduces plasma triglycerides and fatty acids, and increases plasma glucose and insulin. J Biol Chem 1999;274:26761–26766
9. Bessi VL, Labbé SM, Huynh DN, et al. EP 80317, a selective CD36 ligand, shows cardioprotective effects against post-ischaemic myocardial damage in mice. Cardiovasc Res 2012;96:99–108
10. Greenwalt DE, Lipsky RH, Ockenhouse CF, Ikeda H, Tandon NN, Jamieson GA. Membrane glycoprotein CD36: a review of its roles in adherence, signal transduction, and transfusion medicine. Blood 1992;80:1105–1115

11. Kashiwagi H, Tomiyama Y, Honda S, et al. Molecular basis of CD36 deficiency. Evidence that a 478C—>T substitution (proline90—>serine) in CD36 cDNA accounts for CD36 deficiency. J Clin Invest 1995;95:1040–1046
12. Kashiwagi H, Tomiyama Y, Nozaki S, et al. Analyses of genetic abnormalities in type I CD36 deficiency in Japan: identification and cell biological characterization of two novel mutations that cause CD36 deficiency in man. Hum Genet 2001;108:459–466
13. Iizuka Y, Gotoda T, Ishibashi S, Yamada N. CD36 deficiency and insulin resistance. Lancet 2001;358:243
14. Yanai H, Chiba H, Morimoto M, et al. Human CD36 deficiency is associated with elevation in low-density lipoprotein-cholesterol. Am J Med Genet 2000;93:299–304
15. Miyaoka K, Kuwasako T, Hirano K, Nozaki S, Yamashita S, Matsuzawa Y. CD36 deficiency associated with insulin resistance. Lancet 2001;357:686–687
16. Okamoto F, Tanaka T, Sohmiya K, Kawamura K. CD36 abnormality and impaired myocardial long-chain fatty acid uptake in patients with hypertrophic cardiomyopathy. Jpn Circ J 1998;62:499–504
17. Tanaka T, Nakata T, Oka T, et al. Defect in human myocardial long-chain fatty acid uptake is caused by FAT/CD36 mutations. J Lipid Res 2001;42:751–759
18. Tanaka T, Sohmiya K, Kawamura K. Is CD36 deficiency an etiology of hereditary hypertrophic cardiomyopathy? J Mol Cell Cardiol 1997;29:121–127
19. Shadid S, Koutsari C, Jensen MD. Direct free fatty acid uptake into human adipocytes in vivo: relation to body fat distribution. Diabetes 2007;56:1369–1375
20. Kihlberg T, Valind S, Längström B. Synthesis of fatty acids specifically labelled with 11C in various positions, including 2H substitution, for in vivo studies of myocardium using PET. Nucl Med Biol 1994;21:1053–1065
21. Zielinski F, Robinson G Jr. Synthesis of high purity ^{11}C labeled palmitic acid for measurement of regional myocardial perfusion and metabolism. Int J Nucl Med Biol 1984;11:121–128
22. Tchoukalova YD, Harteneck DA, Karwoski RA, Tarara J, Jensen MD. A quick, reliable, and automated method for fat cell sizing. J Lipid Res 2003;44:1795–1801
23. Allred CC, Krennmayr T, Koutsari C, Zhou L, Ali AH, Jensen MD. A novel ELISA for measuring CD36 protein in human adipose tissue. J Lipid Res 2011;52:408–415
24. Ali AH, Koutsari C, Mundi M, et al. Free fatty acid storage in human visceral and subcutaneous adipose tissue: role of adipocyte proteins. Diabetes 2011;60:2300–2307
25. Miles JM, Ellman MG, McClean KL, Jensen MD. Validation of a new method for determination of free fatty acid turnover. Am J Physiol 1987;252:E431–E438
26. Persson X-MT, Blachnio-Zabielska AU, Jensen MD. Rapid measurement of plasma free fatty acid concentration and isotopic enrichment using LC/MS. J Lipid Res 2010;51:2761–2765
27. Shadid S, Jensen MD. Pioglitazone increases non-esterified fatty acid clearance in upper body obesity. Diabetologia 2006;49:149–157
28. Fox KA, Abendschein DR, Ambos HD, Sobel BE, Bergmann SR. Efflux of metabolized and nonmetabolized fatty acid from canine myocardium. Implications for quantifying myocardial metabolism tomographically. Circ Res 1985;57:232–243
29. Bergmann SR, Weinheimer CJ, Markham J, Herrero P. Quantitation of myocardial fatty acid metabolism using PET. J Nucl Med 1996;37:1723–1730
30. Patlak CS, Blasberg RG. Graphical evaluation of blood-to-brain transfer constants from multiple-time uptake data. Generalizations. J Cereb Blood Flow Metab 1985;5:584–590
31. Koutsari C, Mundi MS, Ali AH, Jensen MD. Storage rates of circulating free fatty acid into adipose tissue during eating or walking in humans. Diabetes 2012;61:329–338
32. Koutsari C, Ali AH, Mundi MS, Jensen MD. Storage of circulating free fatty acid in adipose tissue of postabsorptive humans: quantitative measures and implications for body fat distribution. Diabetes 2011;60:2032–2040
33. Jensen MD, Hensrud D, O'Brien PC, Nielsen S. Collection and interpretation of plasma leptin concentration data in humans. Obes Res 1999;7:241–245
34. Fukuchi K, Nozaki S, Yoshizumi T, et al. Enhanced myocardial glucose use in patients with a deficiency in long-chain fatty acid transport (CD36 deficiency). J Nucl Med 1999;40:239–243
35. Kintaka T, Tanaka T, Imai M, Adachi I, Narabayashi I, Kitaura Y. CD36 genotype and long-chain fatty acid uptake in the heart. Circ J 2002;66:819–825
36. Hajri T, Hall AM, Jensen DR, et al. CD36-facilitated fatty acid uptake inhibits leptin production and signaling in adipose tissue. Diabetes 2007;56:1872–1880
37. Bonen A, Han XX, Habets DD, Febbraio M, Glatz JF, Luiken JJ. A null mutation in skeletal muscle FAT/CD36 reveals its essential role in insulin- and AICAR-stimulated fatty acid metabolism. Am J Physiol Endocrinol Metab 2007;292:E1740–E1749
38. Wisneski JA, Gertz EW, Neese RA, Mayr M. Myocardial metabolism of free fatty acids. Studies with 14C-labeled substrates in humans. J Clin Invest 1987;79:359–366
39. Glatz JFC, Luiken JJFP, Bonen A. Membrane fatty acid transporters as regulators of lipid metabolism: implications for metabolic disease. Physiol Rev 2010;90:367–417
40. Drover VA, Nguyen DV, Bastie CC, et al. CD36 mediates both cellular uptake of very long chain fatty acids and their intestinal absorption in mice. J Biol Chem 2008;283:13108–13115
41. Koutsari C, Mundi MS, Ali AH, Patterson BW, Jensen MD. Systemic free fatty acid disposal into very low-density lipoprotein triglycerides. Diabetes 2013;62:2386–2395
42. Goudriaan JR, Dahlmans VEH, Teusink B, et al. CD36 deficiency increases insulin sensitivity in muscle, but induces insulin resistance in the liver in mice. J Lipid Res 2003;44:2270–2277
43. Furuhashi M, Ura N, Nakata T, Shimamoto K. Insulin sensitivity and lipid metabolism in human CD36 deficiency. Diabetes Care 2003;26:471–474